Stoichiometry of LTβR Binding to LIGHT

John Eldredge,[‡] Steven Berkowitz,[‡] Alan F. Corin,[‡] Eric S. Day,[‡] David Hayes,[§] Werner Meier,[‡] Kathy Strauch,[‡] Mohammad Zafari,[‡] Madhavi Tadi,[‡] and Graham K. Farrington*[,‡]

Biogen Idec, Inc., 12 Cambridge Center, Cambridge, Massachusetts 02142, and Boston Biomedical Research Institute, 64 Grove Street, Watertown, Massachusetts 02472

Received February 1, 2006; Revised Manuscript Received June 7, 2006

ABSTRACT: LTβR is a member of the TNF receptor family of proteins. It binds to two different cell surface ligands, LIGHT, a homotypic trimer, and LTα1β2, a heterotypic trimer. We have measured the affinities of the dimeric IgG fusion protein, LTβRIgG, and monomeric LTβR protein binding to both LIGHT and LTα1β2 using surface plasmon resonance and found values of <0.1 and 38 nM for LIGHT and <0.1 and 48 nM for LTα1β2, respectively. We also determined the stoichiometries of binding for both forms of the receptor LTβRIgG and LTβR binding to LIGHT. The data obtained from several biophysical methods are consistent with receptor polypeptide to trimeric ligand ratios of 2:1. The determined masses of the complexes using SEC−LS corresponded to a single LTβRIgG bound to a LIGHT trimer, or two LTβR bound per LIGHT. Sedimentation velocity of varied ratios of LTβR to a fixed concentration of LIGHT were analyzed by SEDANAL and were successfully fit with a model with two tight binding sites on LIGHT and one poor affinity site. Isothermal calorimetric titration of LIGHT with either LTβR or LTβRIgG also demonstrated stoichiometries of 1:2 and 1:1, respectively. The binding of LTβR to LIGHT was endothermic and, hence, entropy-driven. TNFR p55 (extracellular domain) complexed with the trimeric ligand, TNFβ, exhibits a 3:1 receptor/ligand stoichiometry. This complex has been used as the prototypical model setting the receptor−ligand complexation paradigm for the entire TNF family. The LTβR/LIGHT binding stoichiometry of 2:1 demonstrated here does not fit the paradigm. This has numerous implications for cell biology including signaling requiring only dimerization of LTβR rather than trimerization as expected from the structural paradigm.

LTβR[1] (lymphotoxin-β receptor) is a member of the Tumor Necrosis Factor (TNF) receptor family of proteins. LTβR binds to two different membrane-bound TNF family ligands: LIGHT (*l*ymphotoxin like, exhibits *i*nducible expression, and competes with HSV *g*lycoprotein D (gD) for *H*VEM, a receptor expressed by *T* lymphocytes: TNFSF14) and LTα1β2 (lymphotoxin α1β2) (*1*−*3*). LTα1β2 is the only known heteromeric TNF family ligand and binds only to LTβR (*2*, *4*). LIGHT is the more promiscuous ligand, known to also bind two other receptors, Herpes Virus Entry Mediator (HVEM) and soluble Decoy Receptor 3 (DcR3) in addition to LTβR (*1*, *5*). The biological implications of LIGHT interacting with each of the receptors has been recently reviewed (*6*−*8*). These molecules form part of an intercellular communications network (*8*). The cell type and the temporal expression of each ligand and receptor are central to their biological signaling roles. In humans, LTα1β2 expression is induced by cytokines on T-cells in the peripheral blood (*9*) and in mice on splenic T-cells (*10*) and follicular B-cells (*11*). LIGHT is constitutively expressed by myeloid immature dendritic cells and is inducible on T-cells (*1*, *12*). LTβR is constitutively expressed on fibroblasts, epithelial cells, and myeloid cells (*13*−*15*). Thus, it appears that LTα1β2-LTβR-dependent signaling is from lymphocytes to the surrounding stroma and parenchymal cells (*8*). Blockade of LTα1β2-mediated signaling through LTβR with either anti-LTβR antibodies or LTβRIgG affects the follicular dendritic cells and disrupts the network architecture in the lymphoid organs (*16*−*19*). The binding of LIGHT to the stromally localized LTβR results in biological signaling through the intracellular domains of LTβR (*13*). LIGHT signaling through LTβR is sufficient for LIGHT-mediated apoptosis of tumor cells (*20*). The interaction of LIGHT with HVEM affects signaling in T-cells, where it acts as a costimulatory molecule (*6*, *21*, *22*).

The cocrystal structure of soluble TNFR-1 (p55) bound to TNFβ (Tumor Necrosis Factor β ligand or LTα) has been solved (*23*, *24*) and serves as a structural paradigm for cellular signaling in which three monomeric receptor molecules complex with a homotrimeric ligand. This hexameric

* To whom correspondence should be addressed. E-mail: graham.farrington@biogenidec.com. Phone: (617) 679-3224. Fax: (617) 679-2304.

[‡] Biogen Idec, Inc.

[§] Boston Biomedical Research Institute.

[1] Abbreviations: α1β2, LTα1β2-lymphotoxin; LIGHT, (*l*ymphotoxin like, exhibits *i*nducible expression, and competes with HSV *g*lycoprotein D (gD) for *H*VEM, a receptor expressed by *T* lymphocytes: TNFSF14); LTβR, lymphotoxin-β receptor; SEC, size-exclusion chromatograpy; *S*, apparent sedimentation coefficient; SEC−LS, size-exclusion chromatography with in-line light scattering; TNF, Tumor Necrosis Factor; HVEM, Herpes Virus Entry Mediator; DcR3, soluble decoy receptor 3; LTβRIgG, human lymphotoxin-β receptor fused to a hIgG Fc domain; SPR, surface plasmon resonance; FACS, cell-based fluorescent assay; ITC, isothermal titration calorimetry; AUC, analytical ultracentrifugation.

10.1021/bi060210+ CCC: $33.50
Published on Web 08/01/2006

complex is viewed as the competent cell surface complex that signals into cells upon TNF family receptor/ligand binding interactions. Biochemical studies utilizing a variety of analytical techniques such as size-exclusion chromatography with in-line light scattering (SEC−LS) and chemical cross-linking have examined the interaction of either TNF-R1 or TNF-R2 (p75) with the trimeric TNFα ligand. The resulting stoichiometries were between 2:1 and 3:1, respectively (*25*, *26*). Sedimentation equilibrium measurements have strongly suggested a 3:1 stoichiometry of interaction for TNFR1 with the TNFβ ligand (*27*). Crystal structures of the complex between Apo2L and the ectodomain of DR5 (*28*, *29*) and BAFF (B-cell activating factor) with BAFF-R (*30*−*32*) have also revealed 3:1 receptor/ligand molecule stoichiometries. These examples largely support the TNF paradigm that a 3:1 receptor/ligand complex is the basic signaling unit (*31*, *33*, *34*). The only TNF family member receptor known to break the 3:1 receptor-to-ligand paradigm is the interaction of LTβR with LTα1β2 where only two LTβR subunits interact with this heterotrimeric ligand (*3*). For the homotrimeric ligands binding to their receptors, there are no reports of negatively or positively cooperative interactions, suggesting that all receptors bind their target ligand with similar affinity.

In this report, the affinities of LTβR (monomeric soluble human lymphotoxin-β receptor) and LTβRIgG (human lymphotoxin-β receptor fused to a hIgG Fc domain) with the homotrimeric TNF superfamily ligand LIGHT and the heterotrimeric ligand LTα1β2 were assessed using several assay methods, including surface plasmon resonance (SPR), cell-based fluorescent assay (FACS), and isothermal titration calorimetry (ITC). The stoichioimetry of bound LTβR and LTβRIgG to LIGHT was determined by several biophysical methods, including ITC, analytical SEC−LS, and analytical ultracentrifugation (AUC). The interaction of LTβR with LIGHT is consistent with tight binding events for the first two interacting receptors, whereas the third binding event occurs with significantly poorer affinity, if at all. Hence, we propose a model in which a complex of two LTβR molecules bound to a ligand, LIGHT or LTα1β2, accounts entirely for the basic signaling unit.

MATERIALS AND METHODS

Reagents. Endoproteinase Asp-N excision grade was from Calbiochem (San Diego, CA). Protein A fast flow resin was from Amersham Biosciences (Piscataway, NJ). SDS−PAGE gradient gels 4−20% were from Daiichi (Tokyo, Japan). SDS−PAGE molecular weight standards were from Invitrogen (Carlsbad, CA).

Expression of Human LIGHT. Plasmid AN049, encoding Flag-(G4S) 3-human LIGHT was constructed containing the N-terminal flag tag, a four-glycine-one-serine linker repeated four times, and amino acids E90−V240 of human LIGHT (*1*). The plasmid contained the α factor secretion signal and the AOX1 promoter that induces expression in *Pichia pastoris* on methanol induction. AN049 was digested with StuI and introduced into *P. pastoris* strain GA115 by electroporation. Colonies were selected on minimal medium lacking histidine. Strain CCM687 expressing Flag-(G4S) 3 LIGHT was chosen as the most productively expressing strain. A 10 mL culture of *P. pastoris* CCM687 was grown overnight at 25 °C in BMGY media, then inoculated into 1 L of BMGY media in an air-shaken Fernbach flask and incubated at 25 °C for 3 days. The BMGY medium contained 1% yeast extract (Difco), 2% peptone (Oxoid), 100 mM potassium phosphate, pH 6.0, 1.35% Yeast Nitrogen Base (Difco), 4×10^{-5}% biotin, and 2% glycerol. The cells were then harvested by centrifugation at 2500*g* for 20 min. The cell pellet was resuspended in 200 mL of BMMY media that contained 2% methanol and transferred to a fresh Fernbach flask covered with cheesecloth. BMMY medium contained, per liter, 1% yeast extract (Difco), 2% peptone (Oxoid), 100 mM potassium phosphate, pH 6.0, 1.35% Yeast Nitrogen Base (Difco), with 5−10% biotin, and the 2.0% methanol. Incubation was continued at 25 °C for 2 days with shaking, then centrifuged at 2500*g* for 20 min and the supernatant collected and frozen until purification.

Purification of LIGHT and LTα1β2. Pichia-expressed LIGHT was deglycosylated by adding 0.25 mL of 1×10^6 units/mL of Endo H from New England Biolabs (Ipswich, MA) to 1.6 L *of Pichia* supernatant, which was then dialyzed overnight at 4 °C against 2 × 10 L of 20 mM Tris-HCl, pH 8.0. The dialysate was chromatographed on a 2.5 × 8 cm DEAE Sepharose Fast Flow (Amersham Biosciences, Piscataway, NJ) column. The bound protein was eluted with a linear gradient from 0 to 0.4 M NaCl using 30 column volumes. The eluted fractions were analyzed by SDS−PAGE, and those containing LIGHT were pooled and dialyzed overnight at 4 °C in 2 × 1 L of 20 mM sodium acetate buffer, pH 5. The dialysate was chromatographed on a 1.6 × 2.5 cm SP-sepharose Fast Flow (Amersham Biosciences, Piscataway, NJ) column. LIGHT was eluted with a 30 column volume linear gradient of 0 to 0.5 M NaCl. Fractions containing purified LIGHT were identified by SDS−PAGE, pooled, and concentrated to 15 mL by ultrafiltration (Waters, Milford, MA). In three repetitive runs, the concentrate (5 mL each) was loaded onto a HiPrep 26/60 S200 gel filtration column (Amersham Biosciences, Piscataway, NJ) and eluted in PBS, pH 7.5, and fractions containing pure LIGHT, as determined by SDS−PAGE, were pooled. The protein was aliquoted and frozen at −80 °C until use. LTα1β2 was purified as described by Browning et al. (*35*). N-Terminal sequencing was carried out on an Applied Biosystems Procise 494 HT Sequencer. Proteins were analyzed by mass spectra on an LCZ mass spectrometer after deglycosylation with PNGaseF by reduction with DTT and incubation for 12 h at room temperature.

Purification of LTβRIgG and LTβR. The fusion of the human lymphotoxin receptor to human Fc domain (LTβRIgG) was constructed, purified, and expressed as previously described (*2*, *36*). LTβR was cleaved from LTβRIgG as follows. To 1 mL of LTβRIgG at 10 mg/mL (in 20 mM citrate and 10% sucrose, pH 6.7) was added 0.2 μg of Asp-N endoproteinase (35 units/μg). The mixture was allowed to incubate at room temperature for 18−20 h. The reaction was stopped by the addition of $^1/_{10}$ volume of 10 mM EDTA in PBS (pH 7.4). LTβR was obtained by flowing the mixture over a protein A Sepharose (3 mL) column. The column flowthrough containing the LTβR was pooled and dialyzed against 2 × 1 L of 20 mM Tris, pH 8.0, overnight. The LTβR was then chromatographed on a 1.6 × 2.5 cm DEAE column and eluted with a linear NaCl gradient from 0 to 0.5 M NaCl in 30 column volumes. The fractions containing LTβR by

SDS−PAGE were pooled and concentrated to 10 mg/mL using a Biomax spin concentrator with a 10 kDa cutoff (Millipore Corp., Billerica, MA). The concentrated protein was chromatographed on a Superdex 75 column (2.0 × 100 cm), pre-equilibrated in phosphate-buffered saline, pH 7.2. Peak fractions were analyzed by SDS−PAGE and analytical gel filtration for purity and pooled for use.

Determination of Protein Molar Extinction Coefficients. The extinction coefficients of each purified protein were evaluated based on the method of Edelhoch (*37*) as outlined by Pace et al. (*38*). The determined extinction coefficients were used to calculate all protein concentrations. When this method is used, the extinction coefficients for the proteins are as follows (in absorbance units, mg^{-1} cm^{-1}) LTβR, 0.838; LTβRIgG, 1.21; LIGHT, 1.77.

Biotinylation of Reagents. Proteins were biotinylated using the protocol in the Mini-Biotin-XX protein labeling kit (Molecular Probes, Eugene, OR). Briefly described, to 0.5 mg of LTβRIgG in PBS at 5 mg/mL was added 0.05 mL of 1 M $NaHCO_3$, then 25 μL of the biotin-XX reagent was added, incubated with stirring 1 h at room temperature, and then dialyzed into desired buffer overnight at 4 °C.

FACS Assays and Analysis. FACS binding assays using flow cytometry were done according to the method previously described (*39*). Briefly, in direct binding assays, human LTα1β2 was detected on phorbol myristate acetate-activated II-23 cells (American Type Culture Collection (ATCC) Manassas, VA) in FACS buffer with varied concentrations of either the LTβRIgG or biotinylated LTβRIgG (bLTβRIgG). Cells were incubated on ice for 1−2 h, then washed with PBS, and centrifuged. The appropriate steptavidin phycoerythrin- or anti-hFc phycoerythrin-labeled secondary (Molecular Probes, Eugene, OR) in FACS buffer was added, incubated with the cells for an additional 1 h, and washed again. The fluorescent staining of the cellular-bound LTβRIgG on the II-23 cells was quantified by determining the mean channel fluorescence by FACS. Competitive FACS assays were done by the same protocol except the binding of a fixed concentration of biotinylated LTβRIgG was competed with titrations of the desired LTβR reagent for at least 1 h on ice and quantified as before. Cellular flouresence was determined on FACScan equipped with Cellquest software (Becton-Dickinson, Franklin Lakes, NJ). The data were plotted as a function of mean channel fluorescence versus the concentration of the receptor. K_D and IC_{50} values were determined from the half-maximal values of four-parameter fits of the data using Delta Graph (Red Rock Software, Salt Lake City, UT).

Biacore Surface Preparation. SPR studies were performed using a Biacore 3000 instrument (Biacore, Inc., Piscataway, NJ). LTβRIgG was immobilized on CM5 sensorchips using the Biacore amine coupling kit according to manufacturer's instructions. Briefly, the chip was activated with a 50 μL injection of 1:1 *N*-hydroxsuccinimide (NHS)/1-ethyl-3(3-dimethylaminopropyl)-carbodiimide hydrochloride (EDC). A 50 μL sample of LTβRIgG, diluted to 50 μg/mL in 10 mM sodium acetate, pH 5.0, was injected over one quadrant of the activated chip. A second quadrant was exposed to 10 mM sodium acetate, pH 5.0, as a control surface. Excess free amine groups were capped with a 50 μL injection of 1 M ethanolamine. Surfaces were conditioned with 5 × 30 μL injections of 10 mM NaH_2PO_4. Typical immobilization levels were 5000 RU. All samples were prepared in Biacore buffer (10 mM HEPES, pH 7, 150 mM NaCl, 3.4 mM EDTA, 0.005% p-20 detergent, and 0.1% BSA). This same buffer was used as the running buffer during sample analysis. For immobilizations, the same Biacore buffer without BSA was used as the running buffer.

Solution-Phase Biacore Binding Assays. LIGHT or LTα1β2 and receptor were mixed in various ratios in Biacore buffer and incubated at 4 °C for a minimum of 3 h. A 150 μL sample of these solutions was then injected at 10 μL/min over a LTβRIgG-derivatized surface or an underivatized surface as a background control, followed by a 3 min dissociation in Biacore buffer. The surface was regenerated with 2 × 20 μL injections of 10 mM NaH_2PO_4 following each sample injection. When these experimental conditions are used, the binding is mass-transport-limited during approximately the first minute of binding. The mass-transport-limited region was determined from the region of the sensorgrams where the slope of the first derivative plot is zero. During the mass-transport-limited binding phase, the initial rate of binding (V_i) is proportional to the concentration of free ligand in solution. Only free LIGHT should bind to the LTβRIgG surface at these concentrations; therefore, the method measures the concentration of free LIGHT in each solution. The interaction affinity of ligand and receptor in solution was determined by plotting the (V_i) versus the concentration of the varied component in each mixture and fitting the data to the following quadratic equation (*40*) that has the K_D and stoichiometric ratio (n) as variables:

$$V_i/m = [\mathrm{LIGHT}]_f = 1/2([\mathrm{LIGHT}]_t - \{(n[\mathrm{R}]_t + [\mathrm{LIGHT}]_t + K_D) - \sqrt{[(n[\mathrm{R}]_t + [\mathrm{LIGHT}]_t + K_D)^2 - (4n[\mathrm{R}] + [\mathrm{LIGHT}]_t)]}\})$$

Where V_i = initial rate of binding, m = slope of the LIGAND standard curve, $[\mathrm{LIGHT}]_f$ = free LIGAND concentration, $[\mathrm{LIGHT}]_t$ = total LIGAND concentration. and $[\mathrm{R}]_t$ = total receptor concentration.

Analytical Ultracentrifugation. Sedimentation equilibrium and velocity experiments were conducted in a Beckman Optima XL-A or XL-I ultracentrifuge (Beckman, Palo Alto, CA), using an An60 Ti four-hole rotor. All data acquired from these experiments were obtained using the UV−vis absorbance detection system on the ultracentrifuge. Double sector 12 mm charcoal-filled Epon centerpieces were used in velocity experiments, while six-channel, 12-mm, charcoal-filled Epon centerpieces were used in equilibrium experiments. Velocity experiments were conducted at 20 °C at a speed of 40 000 rpm. Equilibrium experiments were conducted at 4 °C over a range of speeds from about 10−30 000 rpm. At the end of the equilibrium experiment, the rotor was accelerated to 40 000 rpm over 12 h and then decelerated to appropriate experimental speeds to record baseline scans. Data from equilibrium experiments were analyzed using the software NONLIN (*41*). The apparent sedimentation coefficient distribution information, $c(s)$, was obtained via data analysis using the software program SEDFIT (*42*). Sedimentation velocity data was analyzed using SEDANAL software (*43*). SEDANAL performs a nonlinear least-squares fit (simplex or Levenberg−Marquardt algorithm) between time-differenced sedimentation velocity data and ideal

sedimentation velocity profiles generated using the finite element method of Claverie (*44*, *45*) implementing kinetic or equilibrium mass action equations for a wide range of user-definable stoichiometric models essentially according to the general procedure of Todd and Haschemeyer (*46*).

Size-Exclusion Chromatagraphy with Light Scattering (SEC−LS) Assays. Size-exclusion chromatography (SEC) was carried out on a Toso Haas SW3000 column (Montgomeryville, PA) in 20 mM sodium phosphate, pH 7.2, and 150 mM NaCl (PBS) at a flow rate of 0.6 mL/min using a Waters Alliance instrument. In addition to UV detection, the eluent was monitored with a refractive index detector (Waters, Milford, MA). Light scattering was monitored using a Precison Detector PD2000 in tandem with a PD2000/DLS from Precision Detectors (Bellingham, MA). Molecular weight determination of each complex was determined using the Precision Detector Software. Analytical gel filtration of either LTβRIgG/LIGHT or LTβR/LIGHT were mixed with the molar molecular ratios indicated in the figure legend. Ratios are relative to the fixed concentration of LIGHT in all samples of 2 μM, in a final injected sample volume of 50 μL.

Titration Calorimetry. Isothermal titration microcalorimetry reactions were performed using a model VP ITC microcalorimeter from Microcal, Inc. (Northampton, MA), stirring at 270 rpm at 25 °C. In individual titrations, 4 μL of the appropriate receptor was added using a computer-controlled 250 μL microsyringe at an interval of 5 min into a cell containing the ligand solution (the cell volume was 1.43 mL). Both receptor and ligand were dialyzed into an identical buffer of 20 mM sodium phosphate and 150 mM NaCl, pH 7. Control experiments were performed by making identical injections of receptor into a cell containing buffer with no protein to correct for small heats of dilution. The experimental data were fitted to a theoretical titration curve using software supplied by Microcal, with ΔH (enthalpy change in kcal mol^{-1}), K_a (association constant in M^{-1}), and n (number of receptor binding sites/trimer ligand molecule) as adjustable parameters. The cell constant, $c = K_a M_t(0)$, where $M_t(0)$ is the initial macromolecule concentration, is of importance in microcalorimetry (*47*) for defining the range over which meaningful measurements of K_a can be made. Experiments to determine K_a were done with c values of $1 < c < 200$. The instrument calibration was checked prior to measurement using standard pulses provided by Microcal's software.

The cumulative heat of binding in a reaction is described by the following eq 1, the multiple independent sites model, which describes the total heat evolved Q for the total sum of the individual reactions, where V_0 is the cell volume, ΔH_t is the enthalpy of binding per mole of ligand, K_{ai} is the binding constant for each binding site, and [L] is the free ligand concentration:

$$Q = V_0[\mathrm{M}]_t \sum (n_i \Delta H_t \mathrm{K}_{ai}[\mathrm{L}])/(1 + K_{ai}[\mathrm{L}]) \qquad (1)$$

To determine the values of n, K_a, and ΔH, the equation above is represented in terms of the binding constant and total ligand concentration $[\mathrm{L}]_t$ to obtain the following quadratic eq 2:

$$Q = (n[\mathrm{M}]_t \Delta H V_0)/2\{1 + [\mathrm{L}]_t/(n[\mathrm{M}]_t) + 1/(nK_a[\mathrm{M}]_t) - [(1 + [\mathrm{L}]_t/(n[\mathrm{M}]_t) + 1/(nK_a[\mathrm{M}]_t))^2 - 4[\mathrm{L}]_t/(n[\mathrm{M}]_t)]^{1/2}\} \qquad (2)$$

The program then uses the standard Marquardt method with routines provided by the ORIGIN software to optimize for n, K_a, and ΔH_b. The thermodynamic parameters were calculated from the eq 3,

$$\Delta G^\circ = \Delta H^\circ - T\Delta S^\circ = -RT \ln K_a \qquad (3)$$

where ΔG, ΔH, and ΔS are the changes in free energy, enthalpy, and entropy of binding, respectively. T is the absolute temperature (Kelvin), and the universal gas constant $R = 1.90$ kcal mol^{-1} K^{-1}.

RESULTS

Determination of the Binding Affinities of LTβR and LTβRIgG to LIGHT and $\alpha 1\beta 2$. LIGHT was expressed as a secreted protein in *P. pastoris*. Following deglycosylation in the supernatant with endo H, LIGHT was purified from the supernatant using three chromatographic steps: DEAE and *S*-sepharose ion exchange followed by gel filtration. Figure 1, lane 1 shows SDS−PAGE analysis of the purified LIGHT.

Mass spectrometry confirmed that the deglycosylated purified LIGHT monomers had the expected molecular weight of 18,274 Da, and N-terminal sequencing of LIGHT showed an N-terminal sequence starting at aspartate three of the cloned sequence. Attempts to express and purify LTβR, in the absence of a linked Fc domain, were unsuc-

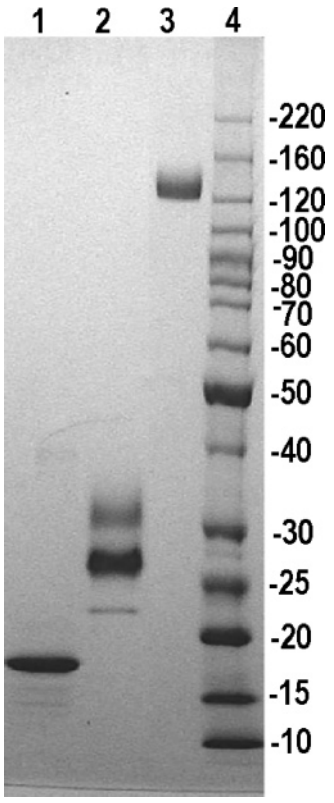

FIGURE 1: Coomassie brilliant blue stained nonreducing SDS 4−20% gradient PAGE of final purified pools of LIGHT (lane 1), LTβR (lane 2), and LTβRIgG (lane 3). Standards are in lane 4; the molecular weights (in kDa) are as indicated to the right of the gel.

Table 1: "Solution-Phase SPR Binding Assay" Apparent K_D Values Determined for LTβRIgG Binding to LIGHT and LTα1β2 and K_D Values Determined for LTβR Binding to LIGHT and LTα1β2, FACS-Determined Apparent K_D Binding Values for LTβRIgG Binding to LTα1β2 on PMA-Activated II-23 Cells, and Competitive IC_{50} Values for LTβRIgG and LTβR versus 1 μg/mL LTβRIgG

	LIGHT	LTα1β2		
	Biacore	Biacore	FACS binding	
	solution binding (nM)	solution binding (nM)	direct (nM)	competition (nM)[a]
LTβR	40 ± 18 (n = 5)	39 ± 17 (n = 5)	(ND)[b]	240 ± 20 (n = 3)
LTβRIgG	<0.10 (n = 3)	<0.10 (n = 3)	1.5 ± 0.6 (n = 4)	28 ± 3 (n = 3)

[a] Versus 1 ug/mL bLTβRIgG. [b] ND, not determined.

cessful due to low expression levels in mammalian cell culture. An alternative proteolytic method was devised to obtain LTβR using the protease Asp-N to cleave the linker between the Fc and LTβR domains of LTβRIgG. AspN was the most convenient protease to use, since the activity could be stopped by the simple addition of EDTA to the solution. SDS−PAGE analysis of the purified preparations is shown in Figure 1. On the basis of peptide mapping, LTβR has varied glycosylation site occupancy on asparagines 13 and 50 (data not shown), resulting in none, one, or two glycans per LTβR molecule which is reflected in the three bands on SDS−PAGE (Figure 1, lane 2). Upon deglycosylation with PNGase F, the LTβR collapses to a single peak at the expected molecular weight of 21,485 Da as determined by mass spectrometry. LTβRIgG, shown in Figure 1 lane 3, was purified as described in Materials and Methods.

Evaluation of the binding affinities of LTβRIgG to LTα1β2 was determined using SPR and cell-based FACS assays. The direct binding of LTβRIgG to LTα1β2, which had been upregulated on the surface of II-23 cells, was measured using a fluorescently labeled secondary anti-Fc polyclonal antibody. The apparent affinity in this assay was determined to be 1.5 nM (Table 1).

To determine affinity constants by SPR, we initially attempted a direct binding of LTβR to LIGHT immobilized on the chip surface. However, we were unable to define conditions that generated a stable surface with immobilized LIGHT. Therefore, we applied the "Solution-phase SPR binding assay" previously used to successfully derive the affinity constants for a similar trimeric ligand (BAFF) and receptor (BAFFR) complex as described by Day et al. (*48*). Described in Materials and Methods are the details of the "Solution-phase SPR binding assay" determination methodology. LTβRIgG was immobilized on an SPR chip that was then used to generate a standard curve in response to free LTα1β2 or LIGHT from 0 to 15 nM. For both LIGHT and LT α1β2, the initial velocity (V_i) versus LTα1β2 or LIGHT response gave a linear response to concentration. The linear V_i to concentration relationship can be used to determine the free LIGHT or LTα1β2 concentrations in reaction

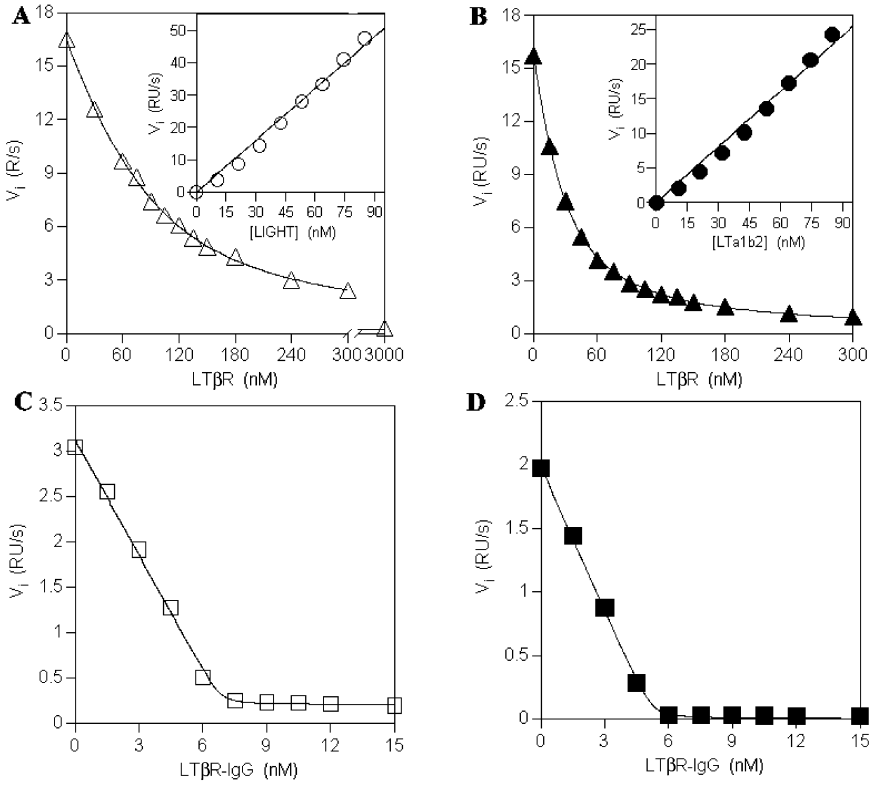

FIGURE 2: Solution-phase binding of LTβR to LIGHT or LTα1β2 and LTβRIgG to LIGHT or LTα1β2. Separate solutions containing the indicated concentrations of (A) (Δ) LTβR with 45 nM LTα1β2, (B) (▲) LTβR with 45 nM LIGHT, (C) (□) 3 nM LTα1β2 with LTβRIgG, or (D) (■) 3 nM LIGHT with LTβRIgG were preincubated for 3 h and then run over a LTβR IgG-derivatized Biacore chip as described in Materials and Methods. The concentrations of free LTα1β2 or free LIGHT in the reaction solutions were determined by reference to a linear standard curve determined from the initial rate of the ligand alone binding to the LTβRIgG-derivatized chip; the linear response curves for LIGHT and LTα1β2 are shown in the inset boxes in panels A and B. The affinities of the solution-phase binding of LTβR or LTβRIgG were determined from the quadratic equation described in Materials and Methods; the fit generated by the equation is shown by the line (−).

mixtures with either LTβRIgG or LTβR. There is no chance for the LTβRIgG on the chip to displace the LTβRIgG or LTβR from a soluble ligand complex because the average contact time of each assay volume flowing over the chip is ~250 ms. The concentrations of free LIGHT mixed in solution with either LTβR or LTβRIgG are shown in Figure 2, panels A and C, respectively, and of free LTα1β2 in solution with either LTβR or LTβRIgG are shown in Figure 2, panels B and D, respectively. Quadratic curve fitting of these curves using the equation in Materials and Methods gives apparent K_D value for the binding affinity of LTβRIgG to LTα1β2 or LIGHT of < 0.1 nM (Table 1). We refer to K_D values for binding of LTβRIgG to LTα1β2 or LIGHT as apparent affinity values due to the avidity component in this binding event. The binding affinities of LTβR to LTα1β2 and LIGHT were determined to be 40 and 39 nM, respectively (Table 1). The K_D value determined by SPR is as much as 15 times lower than the value determined by direct FACS binding. A possible explanation is that the II-23 cells in the FACS assay express surface LTα1β2 in a sufficiently high concentration to cause depletion of the titrated LTβRIgG in the binding reactions. This effect is an important variable to control, especially with molecules having high affinities, as it would artificially raise the determined apparent K_D. To evaluate if the apparent K_D was dependent on the concentrations of expressed LTα1β2, repeating FACS assays were carried out with decreased concentrations of activated II-23 cells. Within experimental error, the same K_D was determined at all II-23 cellular numbers in the assay. Therefore, we attribute differences in the apparent K_D to varied avidity affects that arise from the different assay formats or to affects of post-translation modification of the protein on the surface of the cells.

We also assessed the apparent K_D value for LIGHT binding to LTβRIgG in "Solution-phase SPR binding assay" which, similar to LTα1β2, determined a value of < 0.1 nM (Table 1). To eliminate the avidity affects of the LTβRIgG on K_D, monomeric LTβR was prepared. Using the solution-phase SPR technique, K_D values for the binding of monomeric LTβR to both LIGHT and LTα1β2 were determined to be 40 and 39 nM, respectively (Table 1). These data suggest that presenting the receptor in dimeric rather than monomeric form increases the apparent K_D by >400-fold in this assay system. To evaluate if this large avidity effect is also observed when the ligand is presented on the surface of a cell, we also evaluated the ability of LTβR and LTβRIgG to compete the binding of biotinylated LTβRIgG to LTα1β2 expressed on II-23 cells in the FACS assay. The avidity affect of LTβRIgG was also apparent in the competition assays, with LTβRIgG showing a 9-fold lower IC_{50} compared with LTβR competing biotinylated LTβRIgG binding to cellularly expressed LTα1β2 (Table 1).

SEC−LS Analysis of LIGHT/LTβR Complexes. Before the determination of interaction stoichiometries, the homogeneity of LIGHT, LTβR, and LTβRIgG was analyzed using SEC−LS. LTβRIgG and LIGHT each migrated as a single peak by SEC as shown in Figure 3A and showed no evidence of self-associated multimers, whereas LTβR eluted as a doublet (Figure 3A). Reinjection of either LTβR peak collected from analytical SEC showed that the single peaks do not re-equilibrate back to a doublet (data not shown). Within the limits of SEC−LS analysis, the LTβR peaks had identical

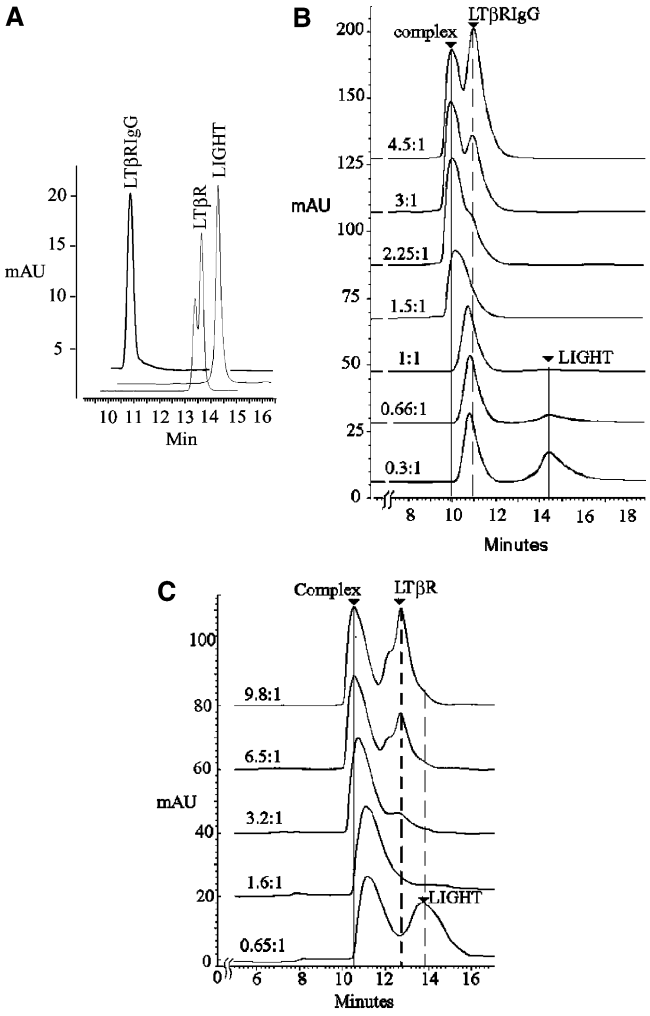

FIGURE 3: (A) Analytical gel filtration of the individual components LTβRIgG, LIGHT, and LTβR are shown in overlay. The LTβR shows two peaks by gel filtration. The *X*-axis represents elution time in minutes and the *Y*-axis the mAU at 280 nM. (B) Analytical gel filtration of LTβRIgG/LIGHT mixtures with the molar molecular ratios indicated, LIGHT concentration was fixed at 2 μM for all experiments. Samples were mixed and incubated for at least an hour prior to injection and chromatography. (C) Analytical gel filtration of LTβR/LIGHT combinations at molar molecular ratios indicated. Additional incubation for up to 24 h had no effect on the traces for LIGHT mixed with either LTβR or LTβRIgG.

molecular weights. Deglycosylation of the isolated individual peaks, with PNGase F followed by mass spectrometry of the respective products, showed the two peaks resulted in identical masses (21,413 Da) equivalent to the predicted mass for LTβR. On the basis of these data, we attribute the two LTβR peaks to differences in glycosylation site occupancy of two, one, or none on the LTβR. No self-associated oligomers of LTβR were observed in the chromatogram.

The stoichiometry of LTβRIgG bound to LIGHT was evaluated by SEC−LS. LTβRIgG was mixed with LIGHT in the ratios indicated in Figure 3B and then subjected to SEC−LS. SEC−LS was used to determine the mass of each of the eluting peaks. The mass data are summarized in Table 2. When the molecular ratios of LTβRIgG to LIGHT were 1:1 or less, the determined mass indicated that one LTβRIgG was bound to each trimeric LIGHT molecule (Table 2). No higher order aggregate complexes were observed. In contrast, when the molar ratio of LTβRIgG to LIGHT exceeded 1:1, the earliest eluting peak representing the complex moved to

Table 2: In-line Light Scattering Data for Peaks Eluting from Gel Filtration Studies[a]

proteins and molar ratio of mixing	determined mL mg^{-1} cm^{-1}	molecular weight from LS	theoretical molecular weight without glycosylation	best fit stoichiometry[b]
LTβRIgG	1.21	100,300	93,700	
LTβR	0.838	25,900[c] (average)	21,829	
LIGHT[d]	1.77	55,900	55,419	
LTβRIgG/LIGHT				
1:1.3		158,000−160,000	149,120	1:1
1.5:1		250,500	242,819	2:1
LTβR/LIGHT				
≥2:1		95,800−96,700	97,420	2:1

[a] The calculated ratios of LIGHT to LTβRIgG or LTβR in each peak are based on the additive masses of individual components as determined by SEC−LS. [b] The calculated ratios of LIGHT to LTβRIgG or LTβR in each peak are based on the additive masses of individual components as determined by the in-line light scattering determination. [c] Average molecular weight of glycosylated LTβR peaks. [d] Molecular weight for the trimeric molecule.

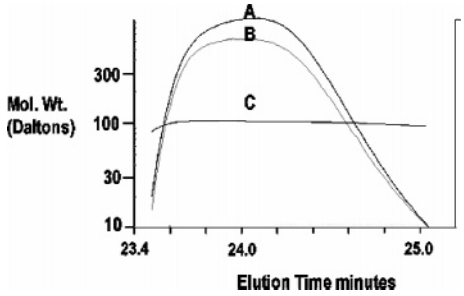

FIGURE 4: Molecular weight analysis of the LTβR/LIGHT complex peak by SEC−LS. LTβR and LIGHT with molecular ratios of 3:1 were combined in a 50 μL sample volume and chromatographed on the HPLC with two SW3000 analytical gel filtration columns linked in tandem. The lead peak eluting from the column corresponded to the appropriate retention time for the LTβR/LIGHT complex and had a peak A_{280} of 0.065 AU. The plot shows three traces analyzed from the LTβR/LIGHT peak. Line A corresponds to refractive index, line B is the 90° light scattering, and line C is the molecular weight calculated using the A and B values. The ordinate corresponds to the molecular weight of the complex in daltons; the ordinate units for lines A and B are not shown.

a shorter retention time (Figure 3B) with a commensurate increase in mass, indicating that now two LTβRIgGs (Table 2) were bound to each LIGHT molecule.

A similar study was performed using LIGHT and monomeric LTβR (Figure 3C). LIGHT combined with low concentrations of LTβR resulted in peaks corresponding to unbound LIGHT and the LIGHT/LTβR complex. As the concentration of LTβR was increased, free LIGHT decreased and a characteristic double peak corresponding to free LTβR was observed. The molecular mass of the peak corresponding to the LTβR/LIGHT complex by light scattering agreed best with a 2:1 complex of LTβR to LIGHT (Figure 3C and Table 2) regardless of the molar ratios employed. This is evidenced from the constant value calculated for the molecular weight from the index of refraction and light scattering data (curve C, Figure 4). Curve C in Figure 4 is flat, indicating that the LTβR complexed with LIGHT is stable during gel filtration and the peak does not represent a distribution of one, two, and three LTβRs bound to LIGHT, in which case the leading and trailing edges of the peak would have been expected to have lower and higher masses, respectively.

Sedimentation Velocity and Sedimentation Equilibrium Analyses. We wanted to characterize the interaction of LTβR with LIGHT at higher concentrations of the ligand and receptor than could be evaluated using the other biophysical techniques we applied. Therefore, we used sedimentation velocity to determine if binding of a third LTβR to LIGHT was detectable at higher concentrations of the receptor/ligand pair. First, at high protein concentrations, the masses of the individual molecules were determined using sedimentation equilibrium and sedimentation velocity experiments to determine if there was concentration-dependent protein dimerization or aggregation. Table 3 reports the calculated molecular weights and determined percent monomer determined by Sedfit and SEDANAL. LTβRIgG, LTβR, and LIGHT all showed excellent fits as single ideal species with the respective expected molecular weights in sedimentation equilibrium or sedimentation velocity.

Next, we did a series of sedimentation velocity experiments using a fixed concentration of LIGHT paired with increasing concentrations of LTβR. Micromolar concentrations of LIGHT and LTβR were used in these experiments to maximize the opportunity to detect any weak binding of LTβR to the third available binding site. First, individual data sets from the individual samples were fit to the model of a single species, holding the molecular weights fixed and floating the density increments. This gave a sedimentation

Table 3: Molecular Weight Determined by Velocity or Sedimentation Equilibrium for Each Individual Species, LTβR, LTβRIgG or LIGHT Determined at Concentrations of 29.8, 9.8, and 18 μM, Respectively, and *S* Values and Standard Deviations (SD) for SEDANAL Single and Global Fits[a]

	Molecular weight			
	Velocity		% monomer	Equilibrium
LTβR	27,400[b]	23,500[c]	99.2[c]	25,200
LTβRIgG	111,000[b]	93,500[c]	99.2[c]	108,100
LIGHT	49,700[b]	53,000[c]	96.2[c]	53,200

S Values and Standard Deviations (SD) for SEDANAL Single and Global Fits

model	single species		two strong, one weak site			
molecule	*S*	SD[d]	complex	*S*	SD[d]	K_{eq}
LTβR (B)	1.31	0.00723	AB	2.577		
LIGHT (A)	2.46	0.00715	ABB	3.22		
			ABBB	3.92	0.0177	8.7×10^4

[a] The lower half of table is the *S* values and standard deviation (SD) for the single fit with SEDANAL to individual molecules and the SEDANAL global fit-to-four ratios of LTBR/LIGHT in Figure 5. [b] Data were fit with SEDANAL. [c] Data were fit with Sedfit. [d] Residuals in AU.

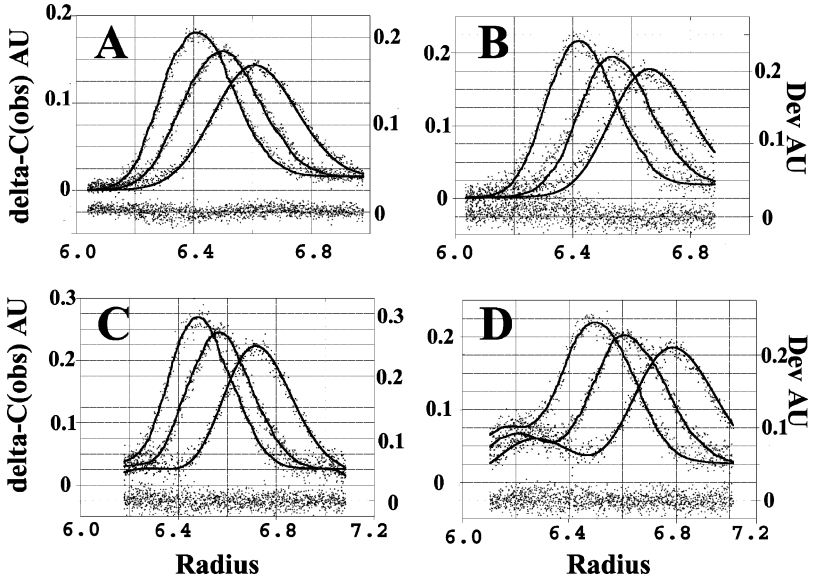

FIGURE 5: A Global fit of 160 total absorbance scans from four separate velocity sedimentation experiments. Each experiment was performed with a fixed concentration of 2 μM LIGHT combined with LTβR at concentrations ratios of (A) 1.5, (B) 2.1, (C) 4.5, and (D) 9 times the LIGHT concentration. Shown for each LIGHT/ LTβR experiment A, B, C, and D are three representative ordered sets out of the 20 sets used in the fit. The solid points are concentration differences, ΔC(obs), at constant radius between two absorbance scans taken at different times. The solid lines are concentration differences, ΔC(calc), calculated from the parameters being fit. The ΔC(obs) and ΔC(calc) correspond to the left *y*-axis in units of absorbance at 280 nm. The plotted deviations between the observed and calculated concentration differences are on the right *y*-axis using the same units and scale (absorbance at 280 nm) but offset to be at the bottom of each plot. The *x*-axis is the radius of the cell in cm and is the same for both *y*-axes.

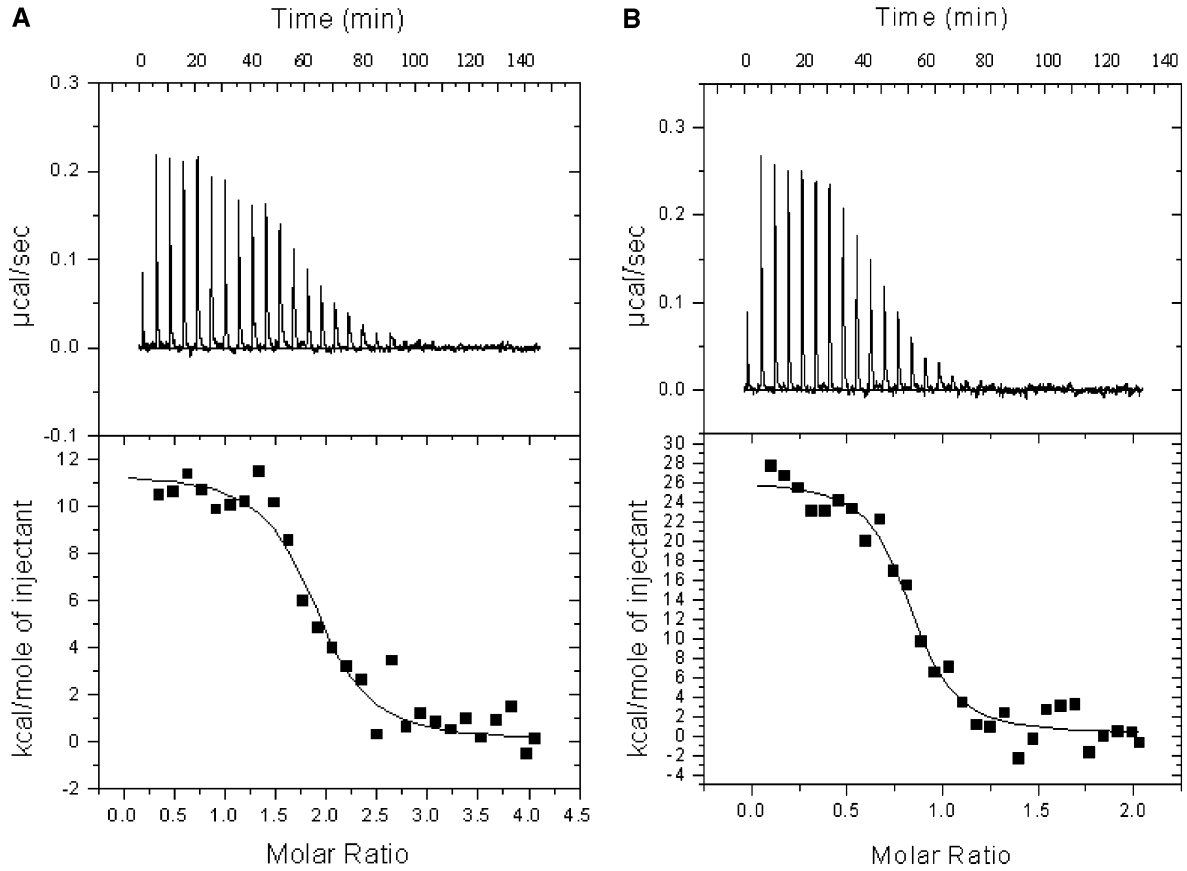

FIGURE 6: Isothermal calorimetric titrations of LIGHT with LTβR. LIGHT (3 μM) in the cell was titrated with either (A) LTβR (150 μM) or (B) LTβRIgG (75 μM) in the syringe. For both A and B, the top shows the time response of heat change upon each addition of receptor. The best fits of the data as judged by comparing Chi-squared statistics for each were achieved using a single site binding model.

coefficient (*S*) value of 1.31 and 2.46 for LTβR and LIGHT, respectively. We then fixed the fitted *S* values, their fitted density increments, the ratio of the mixtures, and weight of the individual components in the global fit and performed a global fit to four data sets of the LIGHT and LTβR mixtures using SEDANAL (Figure 5). The global model fit was A + B = AB, AB + B = ABB, ABB + B = ABBB. The reported *S* values for the reaction components, determined

Table 4: Binding Constants and Thermodynamic Parameters for the Binding of LTβR or LTβRIgG to LIGHT from Isothermal Calorimetric Titrations

	n (sites)	K_D (nM)	ΔH kcal/mol	ΔS cal/mol °K
LTβR	1.88 ± 0.05	126 ± 42	11.5 ± 0.5	69.95
LTβRIgG	0.820 ± 0.019	not valid	26.2 ± 0.9	121.1

K_{eq} for the final LTβR adding to LIGHT, and the standard deviation are in Table 3. In addition, the equilibrium constant for the first two binding events to LTβR was held fixed to the values determined by isothermal calorimetry, and the third value was allowed to float. A global fit using two strong sites and one weak site explains the data with a value for the K_{eq} of the third binding site that would be sufficiently weak that binding of a third LTβR to the LTβR/LIGHT complex would not be detectable in the other techniques evaluated.

Analysis of LTbR and LTbRIgG Binding to LIGHT by Isothermal Titration Calorimetry. We used isothermal titration calorimetry (ITC) to further investigate the stoichiometry and determine the thermodynamics of binding of LTβR and LTβRIgG to LIGHT. Titrations of identical concentrations of LIGHT with either LTβR or LTβRIgG revealed both binding events to be endothermic as evidenced by upward deflections upon individual additions of receptor (top panels of Figure 6, panels A and B, respectively). The individual values for the fitted enthalpies, K_D values, stoichiometry, and calculated entropies for each titration are listed in Table 4. The data for LTβR and LTβRIgG binding to LIGHT were best fit with a single site-binding model that yielded stoichiometry determinations of 1.9 LTβR molecules for the monomeric receptor and 0.82 LTβRIgG molecules for the dimeric receptor per LIGHT trimer. Binding events at only two of the three potential LTβR binding sites on LIGHT were detected in the concentrations used in these experiments. Therefore, either binding to the third site has no detectable associated heat change or no significant binding occurs.

CONCLUSIONS

The prevailing biochemical model for the interaction of TNF family ligands with their target receptor is based on the crystal structure of the soluble human 55 kDa TNF receptor/human TNFβ complex (sTNF-p55/TNFβ) (*23*). In the crystal structure, a TNF-p55 molecule, forming a 3:1 receptor/ligand complex, occupies each of three TNFβ ligand molecule clefts. Banner et al. (*23*) noted that it was "quite possible a two-receptor cluster may be sufficient for TNF signal generation". The crystal structures of the homotrimeric TRAIL ligand showing three DR5 molecules bound (*28*, *33*) and BAFF/BAFF-R in which a 3:1 receptor-to-ligand ratio was observed (*30*−*32*) further support a model where three receptors are bound to a trimeric ligand. The symmetry of the crystal structures suggests a biological model in which each receptor binds with equivalency to each of three identical clefts of a homotrimeric ligand. The identification of a functional LTα1β2, a trimeric ligand containing three asymmetric receptor binding clefts, indicated that functional unsymmetrical receptor/ligand complexes are also possible in the TNF superfamily (*49*). The inability of LTβR to bind to all three clefts of LTα1β2 (*35*) suggests a divalent binding of LTβR to its target ligand is sufficient for intracellular signaling. We conducted extensive solution-based biochemical studies to characterize the binding of monomeric and dimeric forms of LTβR to LIGHT and LTα1β2 to determine if the symmetrical family member LIGHT conforms to the expected paradigm of a 3:1 complex or resembles the heteromeric 2:1 paradigm of LTα1β2.

Using SPR solution binding, we determined the apparent binding affinity of LTβRIgG and the intrinsic binding affinity of LTβR to LIGHT and LTα1β2. At least a 400-fold avidity contribution is observed when comparing the apparent binding affinity of the dimeric LTβRIgG with the intrinsic binding affinity of monomeric LTβR with each ligand. We conclude that the 400-fold increase in the apparent K_D indicates that each LTβR arm of an LTβRIgG binds to two separate clefts on the same ligand, either LTα1β2 or LIGHT (Figure 7A, left cartoon) when receptor and ligand are in a 1:1 complex. No such avidity contribution would be expected if each arm of LTβRIgG were to bind to a single cleft on two independent trimeric ligands in solution (Figure 7, model B). In addition, SEC−LS and sedimentation velocity results of LTβRIgG/LIGHT complexes do not support this mode of interaction in solution. The IC_{50} values of LTβRIgG and LTβR competing with a fixed concentration of biotinylated LTβRIgG to bind LTα1β2 were shown to differ by about 9-fold (Table 1) in a cell-based assay system, using an activated II-23.D7 T cell hybridoma cell line (*36*). The increased IC_{50} value of LTβRIgG over LTβR is also attributed to the avidity of the dimeric form of the LTβRIgG. Notably, depending on the assay system, the apparent avidity contribution of a dimeric form of the receptor can vary between 1 and 2 logs.

We used several biophysical studies techniques to define the interaction of LTβR with LIGHT and determine the receptor/ligand stoichiometric ratio of 2:1. Using SEC−LS, we measured the mass of complexes of LIGHT with either LTβRIgG or LTβR. Mixtures of LTβRIgG and LIGHT at low concentrations gave masses corresponding to 1:1 molar ratios. As the concentrations of LTβRIgG were increased, the mass of the complex corresponded to a 2:1 ratio. However, because the dimeric nature of the LTβRIgG structure, two possible binding models fit these data. In the first model, at high concentration, each LTβRIgG binds with a single arm to LIGHT and the third site remains unoccupied (Figure 7, model B). In the second model (Figure 7, model C), one LTβRIgG is bound in a bidentate manner to LIGHT, while the second LTβRIgG is bound in a one-arm fashion to the remaining third site. To distinguish between the two models, complexes of LTβR and LIGHT were examined in SEC−LS. Even at high concentrations and with a vast excess of LTβR to LIGHT, the mass in SEC−LS always corresponded to two monomeric LTβR molecules bound per LIGHT trimer (Figure 7, model D). These data suggest that, at high concentrations of LTβRIgG, a second LTβRIgG molecule then displaces one arm of the bidendate-bound LTβRIgG as depicted in Figure 7 model B. SEC−LS scattering has been used to determine the stoichiometry for protein−protein interactions with affinities at least as high as 0.2 μM as demonstrated by the nonequilibrium binding gel filtration data showing hFcRn binding to hIgG with a clear 2:1 stoichiometry (*50*). These data indicate that if a

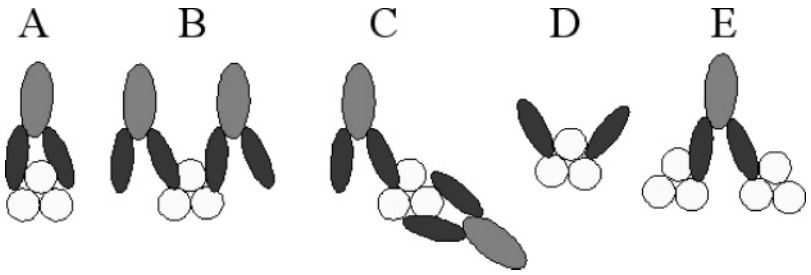

FIGURE 7: Receptor−ligand complex models. (A) A single LTβRIgG bound to LIGHT by both arms; the two-arm binding is reflected in the enhanced binding avidity observed when comparing LTβRIgG and LTβR binding affinities. (B) Two LTβRIgGs bound to a single LIGHT, each by a single arm. (D) The addition of LTβR to LIGHT results in the titration of the first two sites on LIGHT with the third site remaining unoccupied except at very high concentrations of LTβR. (E) LTβRIgG cross-linking of LIGHT was not observed in SEC−LS.

third site on LIGHT is occupied, but not detected, the LTβR would have to bind with a K_D significantly weaker than 0.2 μM.

We used sedimentation velocity to study the complexation of LTβR binding to LIGHT. SEDANAL was used to fit the results and evaluate the ability of various kinetic models to explain the results. Several kinetic models gave reasonable residuals when fit to the experimental data, but were eliminated because the calculated *S* values for the intermediates were unreasonable given the additional mass added for each LTβR added to the LIGHT complex or because the calculated K_{eq} values were inconsistent with results from other binding data. For example, a model in which all three LIGHT binding sites were considered equivalent gave residuals similar to the two tight sites and one loose site model. However, the K_{eq} values returned for such a model suggested that the binding constants were in the micromolar region for all binding events, including the initial binding event of LTβR to LIGHT; a K_{eq} value this high is inconsistent with the SEC−LS, Biacore, and ITC binding data. An attempt to fit the ITC data to a similar three equivalent binding site model resulted in theoretical fits that were clearly incorrect and did not fit the experimental results. The binding model using two tight sites and one weak site best explained the data that resulted in a fit most consistent with the other kinetic binding measurements. The sedimentation velocity results suggest that a third binding event can occur, but that the LTβR affinity for the third site is significantly poorer than the first two binding sites.

The ΔH for LTβR and LTβRIgG binding to LIGHT was determined using ITC. The observed positive reaction heats show that the reaction is an entropically driven binding event. An entropically driven reaction could result from a large overall conformational rearrangement of the LIGHT molecule upon binding of LTβR and/or substantial desolvation of the protein as water molecules are displaced from the LTβR binding interface. The latter hypothesis was offered to explain the entropically driven binding of p75 to NGF (*51*). The titration of LIGHT with LTβR gives a K_D value of 104 nM, a value that is only 2.5-fold different from the value of 38 nM determined by SPR. The low nanomolar affinity value for LTβRIgG binding to LIGHT precludes determining an accurate K_D value by ITC, as this technique is typically limited to K_D determinations >10 nM (*47*, *52*). ITC results support the 2:1 binding model for LTβR and a 1:1 LTβRIgG binding model to LIGHT, with determined stoichiometric values of 1.88 and 0.82, respectively. These results are consistent with the SEC−LS analysis in which molecular masses corresponding to one (Figure 7, model A) or two (Figure 7, models B or C) LTβRIgG molecules bound to a single LIGHT trimer but none corresponding to a polymeric species (Figure 7, model E) were detected. The observation that, at high LTβRIgG/LIGHT ratios, two LTβRIgGs can be bound to a single LIGHT by SEC−LS appears to be inconsistent with the determined LTβRIgG/LIGHT stoichiometry of 1:1 determined in the ITC titration experiments. However, the ratio and concentrations of LTβRIgG to LIGHT were significantly lower for ITC studies than those used for SEC−LS, hence, favoring a 1:1 stoichiometry as depicted in Figure 7A. In addition, a 2:1 versus 1:1 stoichiometry of LTβRIgG binding to LIGHT may not be observed in ITC if the initial binding event involves both arms of a single LTβRIgG to two of the three LIGHT clefts, as shown in Figure 7A. This binding scenario is likely since the LTβRIgG binds with a tighter apparent K_D than LTβR, presumably due to the avidity afforded by the bidentate nature of LTβRIgG binding to LIGHT. At the concentrations used in the ITC experiments, no additional binding events are observed. Using this model, the binding of a second LTβRIgG to the LTβRIgG/LIGHT complex can only occur if a single arm of a second LTβRIgG displaces one arm of the first bound LTβRIgG. If this event were isoenthalpic as expected, it would not be observable by ITC.

We have determined the binding affinities of interaction for monomeric LTβR and dimeric LTβRIgG binding to the heteromeric LTα1β2 and homotrimeric LIGHT ligands. Further, we have shown the stoichiometries of monomeric LTβR and dimeric LTβRIgG bound to LIGHT to be 2:1. LTβR binding to LIGHT, surprisingly, does not fit a 3:1 binding model in which each site would represent an independent and equivalent binding pocket for each receptor ligand binding interaction. All the biophysical techniques employed confirmed that LTβR binds to the homotrimer LIGHT with good affinity at only two of the three potential binding sites. The third site may still bind the receptor, but with an affinity too low to be detectable in the systems employed in these studies. Two of the biophysical techniques employed, sedimentation velocity ultracentrifugation and SEC−LS, are nonequilibrium approaches. Both of these approaches show that LTβR readily occupies the first two sites on LIGHT. No clear, discrete binding event could be assigned to the third site, even at the high micromolar concentrations of protein used in the experiments. On the basis of these data, we suggest a model in which LTβR can readily bind only to two binding sites on LIGHT (Figure 7D). While interaction of LTβR with the third cleft on

LIGHT may occur at high receptor concentrations, this interaction has only been observed at micromolar concentration ranges that would appear to be levels that are too high to be physiologically relevant. Hence, these data suggest that LIGHT-dependent signaling into cells through surface-bound LTβR may occur through dimerization of LTβR receptor molecules on the surface of the cell. The apparent dimerization of LTβR with homotrimeric LIGHT suggests that the current TNF family structural paradigm in which three receptors bind a trimeric ligand for cellular signaling is not universal and certainly not correct for LIGHT and that receptor dimerization as the sole prerequisite for cellular signaling may extend into other homotrimeric TNF family members.

ACKNOWLEDGMENT

The authors thank Drs. Barbara Imperiali and Bob Sauer at MIT for allowing them the use of their XL-A and XL-I ultracentrifuges. We also thank Dr. Walter Stafford for discussions concerning the AUC results.

REFERENCES

1. Mauri, D. N., Ebner, R., Montgomery, R. I., Kochel, K. D., Cheung, T. C., Yu, G. L., Ruben, S., Murphy, M., Eisenberg, R. J., Cohen, G. H., Spear, P. G., and Ware, C. F. (1998) LIGHT, a new member of the TNF superfamily, and lymphotoxin alpha are ligands for herpesvirus entry mediator, *Immunity 8*, 21−30.
2. Crowe, P. D., VanArsdale, T. L., Walter, B. N., Ware, C. F., Hession, C., Ehrenfels, B., Browning, J. L., Din, W. S., Goodwin, R. G., and Smith, C. A. (1994) A lymphotoxin-beta-specific receptor, *Science 264*, 707−710.
3. Ware, C. F., VanArsdale, T. L., Crowe, P. D., and Browning, J. L. (1995) The ligands and receptors of the lymphotoxin system, *Curr. Top. Microbiol. Immunol. 198*, 175−218.
4. Androlewicz, M. J., Browning, J. L., and Ware, C. F. (1992) Lymphotoxin is expressed as a heteromeric complex with a distinct 33-kDa glycoprotein on the surface of an activated human T cell hybridoma, *J. Biol. Chem. 267*, 2542−2547.
5. Montgomery, R. I., Warner, M. S., Lum, B. J., and Spear, P. G. (1996) Herpes simplex virus-1 entry into cells mediated by a novel member of the TNF/NGF receptor family, *Cell 87*, 427−436.
6. Granger, S. W., and Rickert, S. (2003) LIGHT-HVEM signaling and the regulation of T cell-mediated immunity, *Cytokine Growth Factor Rev. 14*, 289−296.
7. Gommerman, J. L. (2004) A role for the lymphotoxin/LIGHT Pathway in T-cell mediated autoimmunity and infectious disease, *Clin. Appl. Immunol. Rev. 4*, 367−393.
8. Ware, C. F. (2005) Network communications: lymphotoxins, LIGHT, and TNF, *Annu. Rev. Immunol. 23*, 787−819.
9. Ware, C. F., Crowe, P. D., Grayson, M. H., Androlewicz, M. J., and Browning, J. L. (1992) Expression of surface lymphotoxin and tumor necrosis factor on activated T, B, and natural killer cells, *J. Immunol. 149*, 3881−3888.
10. Luther, S. A., Bidgol, A., Hargreaves, D. C., Schmidt, A., Xu, Y., Paniyadi, J., Matloubian, M., and Cyster, J. G. (2002) Differing activities of homeostatic chemokines CCL19, CCL21, and CXCL12 in lymphocyte and dendritic cell recruitment and lymphoid neogenesis, *J. Immunol. 169*, 424−433.
11. Worm, M. M., Tsytsykova, A., and Geha, R. S. (1998) CD40 ligation and IL-4 use different mechanisms of transcriptional activation of the human lymphotoxin alpha promoter in B cells, *Eur. J. Immunol. 28*, 901−906.
12. Morel, Y., Schiano de Colella, J. M., Harrop, J., Deen, K. C., Holmes, S. D., Wattam, T. A., Khandekar, S. S., Truneh, A., Sweet, R. W., Gastaut, J. A., Olive, D., and Costello, R. T. (2000) Reciprocal expression of the TNF family receptor herpes virus entry mediator and its ligand LIGHT on activated T cells: LIGHT down-regulates its own receptor, *J. Immunol. 165*, 4397−4404.
13. Murphy, M., Walter, B. N., Pike-Nobile, L., Fanger, N. A., Guyre, P. M., Browning, J. L., Ware, C. F., and Epstein, L. B. (1998) Expression of the lymphotoxin beta receptor on follicular stromal cells in human lymphoid tissues, *Cell Death Differ. 5*, 497−505.
14. Browning, J. L., and French, L. E. (2002) Visualization of lymphotoxin-beta and lymphotoxin-beta receptor expression in mouse embryos, *J. Immunol. 168*, 5079−5087.
15. Stopfer, P., Mannel, D. N., and Hehlgans, T. (2004) Lymphotoxin-beta receptor activation by activated T cells induces cytokine release from mouse bone marrow-derived mast cells, *J. Immunol. 172*, 7459−7465.
16. Mackay, F., and Browning, J. L. (1998) Turning off follicular dendritic cells, *Nature 395*, 26−27.
17. Gommerman, J. L., and Browning, J. L. (2003) Lymphotoxin/light, lymphoid microenvironments and autoimmune disease, *Nat. Rev. Immunol. 3*, 642−655.
18. Cyster, J. G. (1999) Chemokines and cell migration in secondary lymphoid organs, *Science 286*, 2098−2102.
19. Fu, Y. X., and Chaplin, D. D. (1999) Development and maturation of secondary lymphoid tissues, *Annu. Rev. Immunol. 17*, 399−433.
20. Rooney, I. A., Butrovich, K. D., Glass, A. A., Borboroglu, S., Benedict, C. A., Whitbeck, J. C., Cohen, G. H., Eisenberg, R. J., and Ware, C. F. (2000) The lymphotoxin-beta receptor is necessary and sufficient for LIGHT-mediated apoptosis of tumor cells, *J. Biol. Chem. 275*, 14307−14315.
21. Harrop, J. A., McDonnell, P. C., Brigham-Burke, M., Lyn, S. D., Minton, J., Tan, K. B., Dede, K., Spampanato, J., Silverman, C., Hensley, P., DiPrinzio, R., Emery, J. G., Deen, K., Eichman, C., Chabot-Fletcher, M., Truneh, A., and Young, P. R. (1998) Herpesvirus entry mediator ligand (HVEM-L), a novel ligand for HVEM/TR2, stimulates proliferation of T cells and inhibits HT29 cell growth, *J. Biol. Chem. 273*, 27548−27556.
22. Tamada, K., Shimozaki, K., Chapoval, A. I., Zhai, Y., Su, J., Chen, S. F., Hsieh, S. L., Nagata, S., Ni, J., and Chen, L. (2000) LIGHT, a TNF-like molecule, costimulates T cell proliferation and is required for dendritic cell-mediated allogeneic T cell response, *J. Immunol. 164*, 4105−4110.
23. Banner, D. W., D'Arcy, A., Janes, W., Gentz, R., Schoenfeld, H. J., Broger, C., Loetscher, H., and Lesslauer, W. (1993) Crystal structure of the soluble human 55 kd TNF receptor-human TNF beta complex: implications for TNF receptor activation, *Cell 73*, 431−445.
24. D'Arcy, A., Banner, D. W., Janes, W., Winkler, F. K., Loetscher, H., Schonfeld, H. J., Zulauf, M., Gentz, R., and Lesslauer, W. (1993) Crystallization and preliminary crystallographic analysis of a TNF-beta-55 kDa TNF receptor complex, *J. Mol. Biol. 229*, 555−557.
25. Pennica, D., Kohr, W. J., Fendly, B. M., Shire, S. J., Raab, H. E., Borchardt, P. E., Lewis, M., and Goeddel, D. V. (1992) Characterization of a recombinant extracellular domain of the type 1 tumor necrosis factor receptor: evidence for tumor necrosis factor-alpha induced receptor aggregation, *Biochemistry 31*, 1134−1141.
26. Pennica, D., Lam, V. T., Weber, R. F., Kohr, W. J., Basa, L. J., Spellman, M. W., Ashkenazi, A., Shire, S. J., and Goeddel, D. V. (1993) Biochemical characterization of the extracellular domain of the 75-kilodalton tumor necrosis factor receptor, *Biochemistry 32*, 3131−3138.
27. Loetscher, H., Gentz, R., Zulauf, M., Lustig, A., Tabuchi, H., Schlaeger, E. J., Brockhaus, M., Gallati, H., Manneberg, M., and Lesslauer, W. (1991) Recombinant 55-kDa tumor necrosis factor (TNF) receptor. Stoichiometry of binding to TNF alpha and TNF beta and inhibition of TNF activity, *J. Biol. Chem. 266*, 18324−18329.
28. Hymowitz, S. G., Christinger, H. W., Fuh, G., Ultsch, M., O'Connell, M., Kelley, R. F., Ashkenazi, A., and de Vos, A. M. (1999) Triggering cell death: the crystal structure of Apo2L/TRAIL in a complex with death receptor 5, *Mol. Cell 4*, 563−571.
29. Hymowitz, S. G., O'Connell, M. P., Ultsch, M. H., Hurst, A., Totpal, K., Ashkenazi, A., de Vos, A. M., and Kelley, R. F. (2000) A unique zinc-binding site revealed by a high-resolution X-ray structure of homotrimeric Apo2L/TRAIL, *Biochemistry 39*, 633−640.
30. Karpusas, M., Cachero, T. G., Qian, F., Boriack-Sjodin, A., Mullen, C., Strauch, K., Hsu, Y. M., and Kalled, S. L. (2002) Crystal structure of extracellular human BAFF, a TNF family member that stimulates B lymphocytes, *J. Mol. Biol. 315*, 1145−1154.
31. Kim, H. M., Yu, K. S., Lee, M. E., Shin, D. R., Kim, Y. S., Paik, S. G., Yoo, O. J., Lee, H., and Lee, J. O. (2003) Crystal structure of the BAFF−BAFF−R complex and its implications for receptor activation, *Nat. Struct. Biol. 10*, 342−348.

32. Liu, Y., Xu, L., Opalka, N., Kappler, J., Shu, H. B., and Zhang, G. (2002) Crystal structure of sTALL-1 reveals a virus-like assembly of TNF family ligands, *Cell 108*, 383−394.
33. Mongkolsapaya, J., Grimes, J. M., Chen, N., Xu, X. N., Stuart, D. I., Jones, E. Y., and Screaton, G. R. (1999) Structure of the TRAIL-DR5 complex reveals mechanisms conferring specificity in apoptotic initiation, *Nat. Struct. Biol. 6*, 1048−1053.
34. Cha, S. S., Kim, J. S., Cho, H. S., Shin, N. K., Jeong, W., Shin, H. C., Kim, Y. J., Hahn, J. H., and Oh, B. H. (1998) High-resolution crystal structure of a human tumor necrosis factor-alpha mutant with low systemic toxicity, *J. Biol. Chem. 273*, 2153−2160.
35. Browning, J. L., Miatkowski, K., Griffiths, D. A., Bourdon, P. R., Hession, C., Ambrose, C. M., and Meier, W. (1996) Preparation and characterization of soluble recombinant heterotrimeric complexes of human lymphotoxins alpha and beta, *J. Biol. Chem. 271*, 8618−8626.
36. Browning, J. L., Dougas, I., Ngam-ek, A., Bourdon, P. R., Ehrenfels, B. N., Miatkowski, K., Zafari, M., Yampaglia, A. M., Lawton, P., Meier, W., et al. (1995) Characterization of surface lymphotoxin forms. Use of specific monoclonal antibodies and soluble receptors, *J. Immunol. 154*, 33−46.
37. Edelhoch, H. (1967) Spectroscopic determination of tryptophan and tyrosine in proteins, *Biochemistry 6*, 1948−1954.
38. Pace, C. N., Vajdos, F., Fee, L., Grimsley, G., and Gray, T. (1995) How to measure and predict the molar absorption coefficient of a protein, *Protein Sci. 4*, 2411−2423.
39. Force, W. R., Walter, B. N., Hession, C., Tizard, R., Kozak, C. A., Browning, J. L., and Ware, C. F. (1995) Mouse lymphotoxin-beta receptor. Molecular genetics, ligand binding, and expression, *J. Immunol. 155*, 5280−5288.
40. Hulme, E. C., and Birdsall, N. J. M. (1992) *Receptor−Ligand Interactions: A Practical Approach*, IRL Press, Oxford, New York.
41. Johnson, M. L., Correia, J. J., Yphantis, D. A., and Halvorson, H. R. (1981) Analysis of data from the analytical ultracentrifuge by nonlinear least-squares techniques, *Biophys. J. 36*, 575−588.
42. Schuck, P. (2000) Size-distribution analysis of macromolecules by sedimentation velocity ultracentrifugation and lamm equation modeling, *Biophys. J. 78*, 1606−1619.
43. Stafford, W. F., and Sherwood, P. J. (2004) Analysis of heterologous interacting systems by sedimentation velocity: curve fitting algorithms for estimation of sedimentation coefficients, equilibrium and kinetic constants, *Biophys. Chem. 108*, 231−243.
44. Claverie, J. M., Dreux, H., and Cohen, R. (1975) Sedimentation of generalized systems of interacting particles. I. Solution of systems of complete Lamm equations, *Biopolymers 14*, 1685−1700.
45. Claverie, J. M. (1976) Sedimentation of generalized systems of interacting particles. III. Concentration-dependent sedimentation and extension to other transport methods, *Biopolymers 15*, 843−857.
46. Todd, G. P., and Haschemeyer, R. H. (1981) General solution to the inverse problem of the differential equation of the ultracentrifuge, *Proc. Natl. Acad. Sci. U.S.A. 78*, 6739−6743.
47. Wiseman, T., Williston, S., Brandts, J. F., and Lin, L. N. (1989) Rapid measurement of binding constants and heats of binding using a new titration calorimeter, *Anal. Biochem. 179*, 131−137.
48. Day, E. S., Cachero, T. G., Qian, F., Sun, Y., Wen, D., Pelletier, M., Hsu, Y. M., and Whitty, A. (2005) Selectivity of BAFF/BLyS and APRIL for Binding to the TNF Family Receptors BAFFR/BR3 and BCMA, *Biochemistry 44*, 1919−1931.
49. Browning, J. L., Sizing, I. D., Lawton, P., Bourdon, P. R., Rennert, P. D., Majeau, G. R., Ambrose, C. M., Hession, C., Miatkowski, K., Griffiths, D. A., Ngam-ek, A., Meier, W., Benjamin, C. D., and Hochman, P. S. (1997) Characterization of lymphotoxin-alpha beta complexes on the surface of mouse lymphocytes, *J. Immunol. 159*, 3288−3298.
50. Martin, W. L., and Bjorkman, P. J. (1999) Characterization of the 2:1 complex between the class I MHC-related Fc receptor and its Fc ligand in solution, *Biochemistry 38*, 12639−12647.
51. He, X. L., and Garcia, K. C. (2004) Structure of nerve growth factor complexed with the shared neurotrophin receptor p75, *Science 304*, 870−875.
52. Leavitt, S., and Freire, E. (2001) Direct measurement of protein binding energetics by isothermal titration calorimetry, *Curr. Opin. Struct. Biol. 11*, 560−566.

BI060210+